Effect of Glycine on Aggregation of Citrate-functionalised Gold Nanoparticles and SERS Measurements

Maria J. Vesga[1], David McKechnie[1,3], Stacey Laing[2], Hayleigh Kearns[2], Karen Faulds[2], Karen Johnston[1], and Jan Sefcik[1,4]

[1]Department of Chemical and Process Engineering, University of Strathclyde, 75 Montrose Street, Glasgow G1 1XJ, U.K.
[2]Centre for Molecular Nanometrology, WestCHEM, Department of Pure and Applied Chemistry, Technology and Innovation Centre, University of Strathclyde, 99 George Street, Glasgow, G1 1RD, U.K.
[3]Doctoral Training Centre in Continuous Manufacturing and Advanced Crystallisation, University of Strathclyde, Glasgow G1 1RD, U.K.
[4]EPSRC Future Manufacturing Research Hub in Continuous Manufacturing and Advanced Crystallisation, University of Strathclyde, Glasgow G1 1RD, U.K.

March 15, 2021

Abstract

Surface enhanced Raman Scattering (SERS) can be used as a novel way of probing local liquid composition and structure at solid-liquid interfaces. This is particularly important for understanding the mechanism of heterogeneous nucleation from solution, where solutes are present at relatively high concentrations. To obtain information about the solution composition and structure near a gold nanoparticle (AuNP) surface, which facilitates SERS, it is thus necessary to understand the role of the analyte in AuNP aggregation, and its effect on the SERS signal and the Raman signal from the bulk. We have used dynamic light scattering and UV-Vis spectroscopy to investigate how glycine influences the aggregation of citrate-functionalised gold nanoparticles (AuNPs), and thus the SERS response, in glycine aqueous solutions. At pH 4 the AuNP suspensions in aqueous solutions (without glycine) did not aggregate due to the electrostatic stabilisation by negatively charged citrate functional groups. However, the addition of glycine promoted aggregation of the AuNPs, concomitantly increasing the strength of the SERS signal. Under these conditions glycine is zwitterionic, and its effect on the colloidal stability of AuNPs is most likely due to its association with citrate, affecting its charge state, resulting in reduction of the electrostatic stabilisation of the AuNPs. Using SERS as a solid-liquid interface probe provides a window into an interplay of interfacial and colloidal phenomena in the AuNP suspensions.

1 Introduction

Surface enhanced Raman scattering (SERS) uses strong local fields from surface plasmon resonance, typically using gold and silver nanoparticles (NP) as the enhancing surface, to provide vibrational spectral information about molecules near the nanoparticle surface, and hence its concentration and local structure. SERS is usually used to detect molecules at very low analyte concentrations where the analyte has a negligible Raman signal from bulk.

SERS has previously been used to study glycine in aqueous solution, including the effects of pH [1], glycine concentration [2], the difference between gold and silver NPs [3], the effect of gold NP shape and size [4], and the orientation of glycine adsorbed on the gold NP surface [5,6]. These reported SERS spectra of glycine show considerable variation, which is likely due to using NPs of different metals, surface chemistries, shapes, and sizes. The gold and silver NPs used in SERS are typically stabilised with a capping agent which may also be the reducing agent used in the synthesis. For example, the Turkevich synthesis method [7, 8] for gold NPs (AuNPs), caps the AuNPs with a citrate layer, which gives the AuNPs a negative surface charge and stabilises the colloidal suspension. Therefore, in addition to the bulk Raman signal, a signal from NP capping agents e.g. citrate may also be present as well as signals from the analyte. Finally, in order to achieve high enhancement factors in SERS, it is required to aggregate the NPs. NP aggregation is typically achieved by colloidally destabilising the NPs via changing the pH, adding salts e.g. chlorides, nitrates or sulphates, but it can also be achieved by using small organic molecules, which act as bridging linkers promoting the aggregation [9] or by the analyte itself causing the aggregation, which has been harder to control. Therefore, at high concentrations, the analyte itself is likely to promote aggregation of the AuNPs thus impacting the SERS signal.

SERS also has the potential to be used as a novel way of probing local composition and structure at solid-liquid interfaces, where analytes are liquid mixture components present at relatively high concentration. In particular, it can be used to probe the mechanism of heterogeneous nucleation. Crystal nucleation is well known to mainly occur at interfaces e.g. impurities or solid surfaces, and the presence of interfaces has been observed to significantly enhance nucleation rates. Glycine in aqueous solution is an interesting system for investigation of crystal nucleation since glycine forms several crystal polymorphs and exhibits mesoscale clusters in aqueous solutions [10–12]. Glycine typically crystallises as the α-phase in bulk cooling crystallisation under agitation, but the crystal structure formed from heterogeneous nucleation depends on the interface [13–16]. Recent studies of glycine nucleating from aqueous solution have shown that tridecane and PTFE interfaces significantly increased the nucleation rate [17, 18]. Molecular dynamics simulations indicated that there is a significant concentration enhancement and a preferential orientation of glycine at the tridecane interface [18]. In order to fully understand the interfacial effects on the mechanism of heterogeneous nucleation, it is necessary to probe the solution interfacial properties and solute adsorption directly through in situ experimental techniques, such as SERS.

In order to obtain information about the composition and structure of solutions near solid-liquid interface via SERS, it is thus necessary to understand the interplay of the Raman signals from the bulk, the role of the analyte on the NP aggregation, and the effect of the aggregation on the SERS signal of both the analyte and the NP functionalisation. In this work, we use UV-Vis spectroscopy (UV-Vis), dynamic light scattering (DLS), Raman and SERS to investigate how glycine concentration and pH affects the aggregation of citrate-capped AuNPs suspended in glycine aqueous solutions, and how the aggregation influences the SERS signal.

2 Methodology

2.1 Solution preparation

AuNPs of diameter 40 nm were synthesised by using citrate reduction adapted from the Turkevich and Frens method [7, 8]. 500 mL of deionised water (Milli-Q, 18.2 MΩ cm) and 60.5 mg of sodium tetrachloroaurate (III) dihydrate ($AuCl_4Na.2H_2O$, 99% from Sigma) were added to a round bottomed flask and the mixture was stirred using a IKA Stirrer Werke RW 16 basic assembled with a glass link stirrer (speed setting 6) and heated until boiling using a Bunsen burner. A solution of sodium citrate tribasic was prepared by adding 57.5 mg of sodium citrate tribasic dihydrate ($C_6H_5NaO_7.2H_2O$, ACS reagent $\geq$99% from Sigma) to 7.5 ml

of deionised water. This solution was quickly poured into the flask triggering a sudden colour change from light yellow to dark purple. The solution was then boiled for a further 15 minutes before being left to cool for 1 hour whilst stirring. The colloidal solution was stored in dark cupboard at room temperature. The final concentration of AuNPs was calculated to be 6.171×10^{-11} M using reported extinction coefficient data for AuNPs [19, 20].

Stock solutions of glycine with concentrations of 200, 100, 2 and 0.2 g glycine/kg water (referred to hereafter as g/kg water) were prepared at a high temperature (90°C). Solid glycine powder (≥99% electrophoresis from Sigma) and deionised water (Milli-Q, 18.2 MΩ cm) were used. Required amounts of glycine and water were weighed at room temperature, transferred into a 100 mL glass bottle, and sealed. The solution was heated and stirred at 600 rpm for 1 hour at 90°C±1°C using a hotplate magnetic stirrer (IKA RCT Basic) supplied with an external temperature probe. The solutions were left to cool at room temperature. Appropriate aliquots of stock solutions were taken to obtain final concentrations of glycine in gold colloid suspensions of 100, 50, 1 and 0.1 g/kg water. The final concentration of the AuNPs after mixture with the glycine solutions was 3.1×10^{-11} M.

A sodium chloride stock solution (0.2 M) was prepared by adding 292.2 mg of NaCl (ACS reagent ≥99% from Sigma) to 25 ml of deionised water and then appropriate aliquots of this solution and gold colloid were mixed to obtain final sodium chloride concentrations of 0.1 M, 0.01 M and 0.001 M. The final concentration of the AuNPs after mixture with the solutions was 3.1×10^{-11} M.

Prior to the UV-Vis, DLS and SERS measurements, the pH of the glycine solutions, gold nanoparticles and mixtures after glycine addition were measured at room temperature (20°C) using a Jenway 3510 pH meter. The pH of the colloidal AuNP solution after preparation was 4.54. The pH of the AuNP solution was adjusted to 2 and 4 by titration of 1 wt% HCl or to 6 and 8 by titration of 1 wt% NaOH under vigorous stirring conditions. The pH of the glycine/AuNPs mixtures was adjusted to 4 (±0.003) by titration of 1-3 wt% HCl. This variation in the concentration of HCl was required in order to avoid significant changes in the concentration of the final solutions.

2.2 Characterisation

All samples (glycine/AuNPs and pure gold nanoparticles) were analysed after their preparation by UV-Vis, Dynamic Light Scattering (DLS) and SERS. UV-Vis spectra were recorded using an Agilent Cary 60 spectrophotometer. The samples were measured using semi-micro (4.5 cm × 1.25 cm × 1.25 cm, light path 10 mm) methacrylate (PMMA) cuvettes with a sample volume of 1.5 mL. Measurements were made between 200-800 nm with a scan rate of 600 nm/min. Hydrodynamic diameter and zeta potential measurements of gold nanoparticles were carried out using a Zetasizer Nano Series ZEN3500 (Malvern Instruments Ltd.). The hydrodynamic diameter of the samples was measured using macro (4.5 cm × 1.25 cm × 1.25 cm, light path 10 mm) methacrylate PMMA cuvettes with a sample volume of 1 mL. Similar cuvettes with an inserted dip cell were used for zeta potential measurements.

SERS spectra were acquired using a Snowy Range Instrument (model Sierra 2.0). The excitation was a diode laser with excitation wavelength of 785 nm at the maximum output laser power of 78 mW. Spectra were recorded in the range 200-2000 cm^{-1} and an integration time of 5 s. Raman spectra were acquired in glycine solutions using the same equipment. The samples were placed in vials (Merck; screw clear glass vial thread, ID= 854190, O.D.×H×I.D. 14.75 mm × 45 mm × 8 mm, total volume 4 mL). Aliquots of 2 mL of solution were transferred into vials and sealed with lids.

Time-dependent experiments were performed using each technique in order to investigate the colloid

aggregation over time. Therefore, SERS signal changes, UV-Vis extinction spectra kinetics and diameter of aggregates were monitored in each sample at room temperature over 1 hour at intervals of 10 min.

Both the Raman spectra and SERS spectra were processed using Origin and MATLAB. First, a background spectrum of the glass vial and water was subtracted from the Raman and SERS spectra obtained. Some samples were smoothed with up to 30 points. Finally, a baseline generated by MATLAB was subtracted from each of the spectra obtained. All the baselines were generated with k=280, where k is the search range of the minimum peaks; similar to the 'period = T' of a sinusoidal function. A demonstration of the baseline correction is shown in the Supporting Information (SI).

3 Results and Discussion

3.1 Effect of pH on aggregation of AuNPs

In this section we explore the effects of pH on AuNP aggregation in aqueous solution using UV Vis spectroscopy. We identify pH values where aggregation does not occur, and later use this pH to determine how glycine concentration affects AuNP aggregation. The as-prepared, non-aggregated AuNP suspension at pH 4.54, had AuNP colloids with mean hydrodynamic diameter of 52.5±1 nm and the zeta potential were measured to be -37.1±0.5 mV.

Figure 1 shows the UV Vis extinction spectra and the hydrodynamic diameter of the as-prepared AuNP colloidal suspension at a concentration of 6.2×10^{-11} M at its as synthesised pH of 4.54 and at pH values of 2, 4, 6 and 8. The spectrum for pH 4.54 shows a peak at 530 nm, which is similar to the calculated light extinction at 535 nm reported for AuNPs with diameters between 20 and 40 nm [19, 20].

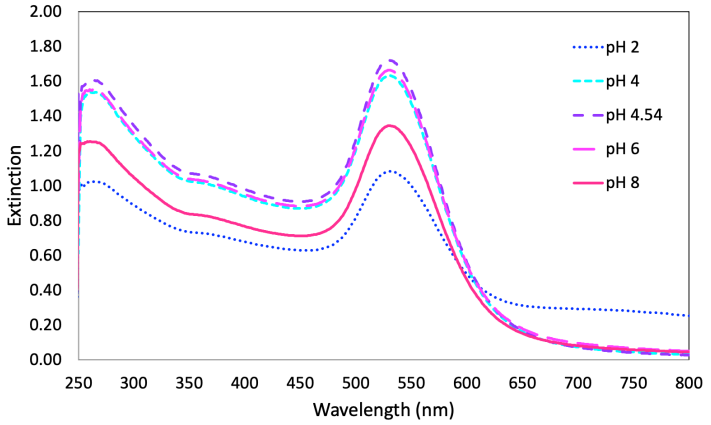

pH	Hydrodynamic diameter (nm)
2	70
4	53
4.54	52
6	51
8	54

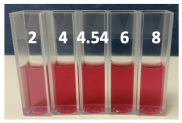

Figure 1: UV Vis extinction spectra of AuNPs dispersions with a concentration of 6.2×10^{-11} M at different pH values (2, 4, 6, 8) after 60 min and of as synthesised AuNPs at a pH of 4.54 at 0 min. The table shows the hydrodynamic diameter of the AuNPs at the different pHs. The photo of vials of AuNP dispersions, shows that at a pH of 2 the dispersions have a pale purple colour, indicating aggregation.

The spectra of the colloidal suspensions at different pH values also exhibit an extinction peak at 530 nm. No changes in peak position are observed for pH 4, 6 and 8, suggesting that AuNPs remain unaggregated. This observation is consistent with the measured mean hydrodynamic diameters, which remain between 51 and 54, similar to that of the pH 4.54 suspension. The pKa values of citrate are 3.13, 4.76 and 6.4. At pH values above the lowest pKa value of 3.13, one, two or all of the carboxyl groups of the citrate-functionalisation

are deprotonated, and the citrate-functionalised NPs have an overall negative charge, promoting their dispersion in the solution. At a pH of 2, a broad band appears at longer wavelengths indicating aggregation of the AuNPs, consistent with the mean hydrodynamic diameter increasing to 70 nm, which is significantly larger than those measured at higher pH. At pH 2, below the lowest pKa value of 3.13, all the carboxyl groups of the citrate are protonated, neutralising the AuNP charge, and hence enabling aggregation due to dispersion forces. The SPR wavelength shifts due to AuNP aggregation, which can also be observed visually by the colour change to a pale purple colour rather than the deeper red of non-aggregated AuNP solutions (see Figure 1 inset).

3.2 Effect of glycine concentration on aggregation

Taking into account that AuNPs did not show aggregation at pH 4 due to their electrostatic stabilisation, we used this pH to study the effect of glycine on AuNP aggregation. Figure 2 shows the UV Vis extinction spectra of AuNPs suspended in solutions of glycine at concentrations of 0.1, 1, 50 and 100 g/kg and for different measurement times.

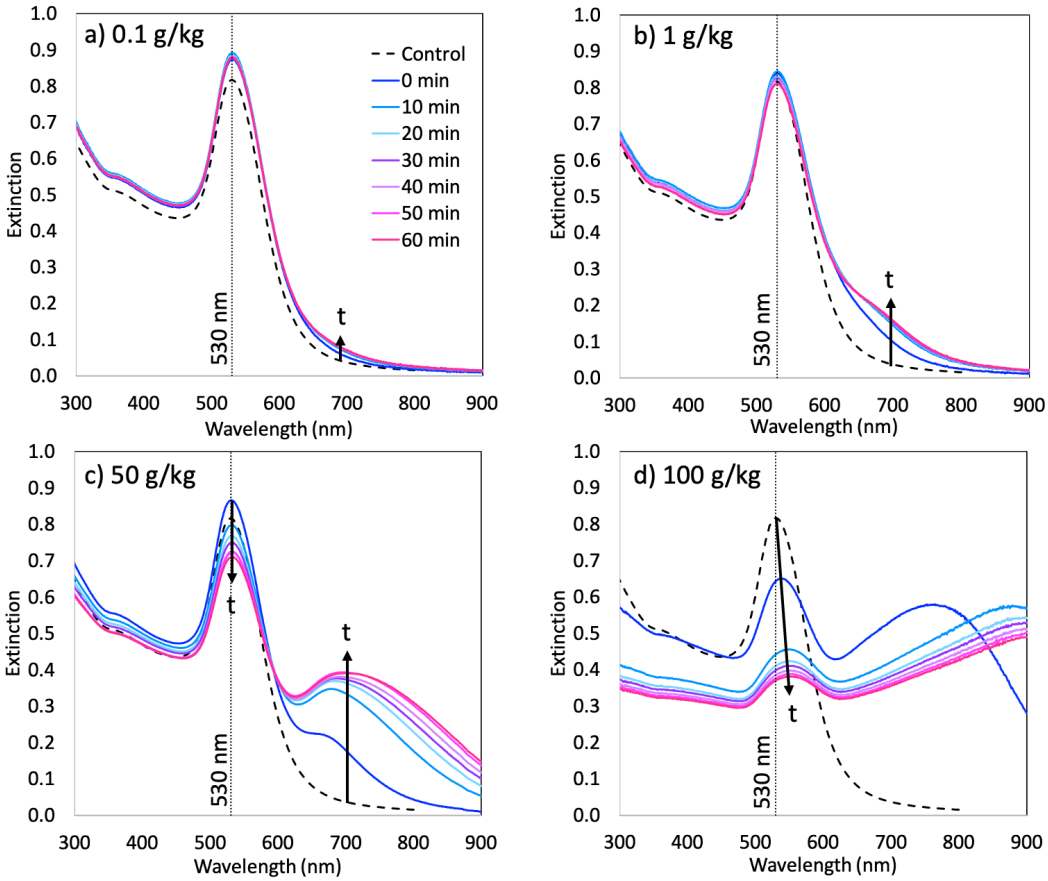

Figure 2: Time-dependent UV Vis spectra of glycine AuNP solutions at an AuNP concentration of 3.1×10^{-11} M at pH 4 and glycine concentrations of a) 0.1, b) 1, c) 50 and d) 100 g/kg. The "control" spectrum is as-prepared AuNPs at 6.2×10^{-11} M and pH 4 without glycine with the extinction halved to account for the different AuNP concentrations.

For the most dilute glycine solution of 0.1 g/kg, shown in Figure 2(a), the UV Vis spectra remain similar to that of the pure AuNP solution, indicating that aggregation is marginal. For concentrations of 1 g/kg

and 50 g/kg, shown in Figures 2(b) and 2(c), respectively, a peak appears between 650 nm and 750 nm, which is indicative of AuNP aggregation. The intensity of this peak sharply increases after 5 min and then plateaus with time while simultaneously shifting slightly towards larger wavelengths. The extinction spectra for a glycine concentration of 100 g/kg, shown in Figure 2(d), shows that the extinction peak at 530 nm significantly decreases in intensity and slightly red-shifts in a time-dependent manner. A second broad peak between 700 and 850 nm appears immediately after mixing, then shifts to higher wavelengths of above 865 nm. After an abrupt increase in intensity in the first 10 minutes, the peak intensity slowly decreases with time. This suggests that the AuNPs quickly aggregate into larger clusters after adding glycine to AuNP suspensions at pH 4, while the decrease in intensity could indicate sedimentation of these large clusters. We note that there is no AuNP aggregation in a 50 g/kg glycine solution at its natural pH of 6.34 even after 30 min (see Supporting Information).

The aggregation of AuNPs for 50 and 100 g/kg is clearly seen by the change in hydrodynamic diameter of the AuNP aggregates, shown in Figure 3 for glycine concentrations of 0.1, 1, 50 and 100 g/kg. At the lower concentration of 0.1 g/kg there is little change in the hydrodynamic diameter suggesting negligible aggregation in agreement with the UV Vis spectra in Figure 2(a). For the 1 g/kg we observe only a marginal increase in the hydrodynamic radius after 60 min, compared to a clear growth in a shoulder in the extinction spectra in Figure 2(b). This shows that the extinction spectra are more sensitive than DLS in measuring marginal aggregation of AuNPs. At the higher concentrations of 50 and 100 g/kg, the diameter increased to around four and six times the original diameter of AuNPs, respectively, directly after mixing the AuNPs and glycine. The hydrodynamic diameter shows a steady increase with time, up to values of around 1000 nm at 60 minutes, revealing that aggregation is still occurring after this time.

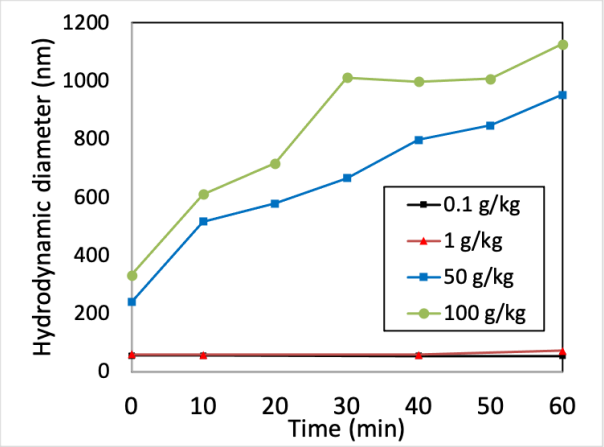

Figure 3: Time evolution of the mean hydrodynamic diameter of AuNP aggregates in solutions with different glycine concentrations of 0.1, 1, 50 and 100 g/kg at pH 4.

These results clearly show that glycine is able to facilitate aggregation of AuNPs. At a pH of 4, glycine is in the zwitterionic form, where the amine group is positively charged but the carboxylic group is negatively charged, therefore the overall charge is neutral [21]. At this pH citrate functionalised nanoparticles are negatively charged and aggregation is observed at glycine concentrations as low as 1 g/kg of water. There are several possible mechanisms how glycine can affect aggregation of AuNPs stabilised by negatively charged citrate groups. Electrostatic repulsion between charged colloidal particles can be screened by adding electrolytes (such as NaCl). While glycine is a zwitterion under the conditions investigated here, it does not act as an electrolyte and it was recently reported that in fact glycine acts to oppose electrostatic screening by salts [22]. Another way to suppress electrostatic repulsion is to reduce the surface charge of AuNPs, which can be achieved by decreasing the charge of adsorbed citrates or by decreasing the surface coverage of citrate on AuNPs. The effect of glycine on citrate dissociation is plausible considering that sodium citrate and

glycine were found to have favourable interactions in aqueous solutions [23]. We note that since the glycine is in zwitterion form, the positive amine group could interact with the negative citrate group, which could change the overall charge distribution near the AuNP surface. We also speculate that it may be possible that glycine competes with citrate for adsorption on AuNP, so that increasing concentration of glycine may lead to partial desorption of citrate and thus decrease the surface coverage of citrates on AuNPs. Regardless of whether glycine affects charge of adsorbed citrates or surface coverage of citrates, it is plausible that increasing the concentration of glycine results in a decreasing surface charge density on AuNPs so that their colloidal stability decreases and the extent of aggregation increases. It has also previously been proposed that glycine acts as a linker between silver colloidal particles prepared with sodium borohydride, facilitating assembly of these nanoparticles as observed by TEM [2].

3.3 Effect of glycine concentration on SERS

SERS uses local surface plasmon resonance from the AuNPs to enhance the Raman signal of molecules near the AuNP surface and is more intense when the AuNPs are aggregated. Given that the UV-Vis and DLS results showed that increasing glycine concentration increases the aggregation of the AuNPs, we expect that the glycine solutions with highest AuNP aggregation will have the strongest SERS intensity. For the highest glycine concentration of 100 g/kg, we note that there is significant sedimentation, which does decrease the SERS intensity with time (see Figure 7). Figure 4 shows both the Raman and SERS spectra for the various concentrations of glycine studied at pH 4.

The Raman spectra of glycine at different concentrations in the absence of AuNPs are shown in Figure 4. For the lowest concentrations of 0.1 and 1 g/kg (Figure 4(c,d)) there is only a weak, broad peak between 1250 and 1450 cm^{-1}. At higher concentrations of 50 and 100 g/kg (Figure 4(a,b)), we observe spectra with well-defined Raman bands, the most intense peaks occurring at 507, 897, 1332 and 1413 cm^{-1}, which have been attributed to CO_2 rocking, CC and CN stretch, CH_2 wag, and CO_2 symmetric stretch modes, respectively [24]. Our Raman frequencies are in agreement with previous literature [4–6, 24, 25].

The SERS spectra, acquired 60 min after mixing the glycine and AuNP solutions, are shown in Figure 4(a-d). The SERS spectra for glycine reported in the literature show considerable variation, which could be due to different glycine concentration and NP metal, functionalisation, shape, and size [1–6]. However, it could also be due to the varying degrees of aggregation of the AuNPs as the glycine concentration used varied from the lowest value of 0.01 mM [5] to the highest value of 1 M [2]. At low glycine concentrations, the contribution from citrate vibrational frequencies could be significant in measured SERS spectra is usually overlooked. This variation in SERS spectra combined with discrepancies in the Raman mode assignments for the neutral glycine molecule in gas phase, and also for zwitterionic glycine in solution [24–28] makes vibrational mode assignments for SERS challenging as well.

We can see in Figure 4(a-d) that the SERS peaks change frequency and intensity as the glycine concentration increases. This variation in SERS spectra with glycine concentration, which could arise due to a combination of Raman scattering from the glycine solution and SERS from glycine on the surface of the nanoparticles, is observed at these very high glycine concentrations. The contribution of the Raman signal to the overall signal will increase with glycine concentration. The SERS signal may also vary with glycine concentration if there are changes in the orientation of glycine on or near AuNPs surface with changing glycine concentration. It would be expected that the Raman signal from the bulk glycine solution would lead to additional peaks at higher concentrations and this does occur, for example the peak at 897 cm^{-1} increases in intensity as glycine concentration increases. However, surprisingly, there are some strong peaks in the low concentration solutions, that diminish or disappear at higher concentrations. The changes in spectra and reduction in intensity of some peaks with increasing glycine concentration means that the SERS signal

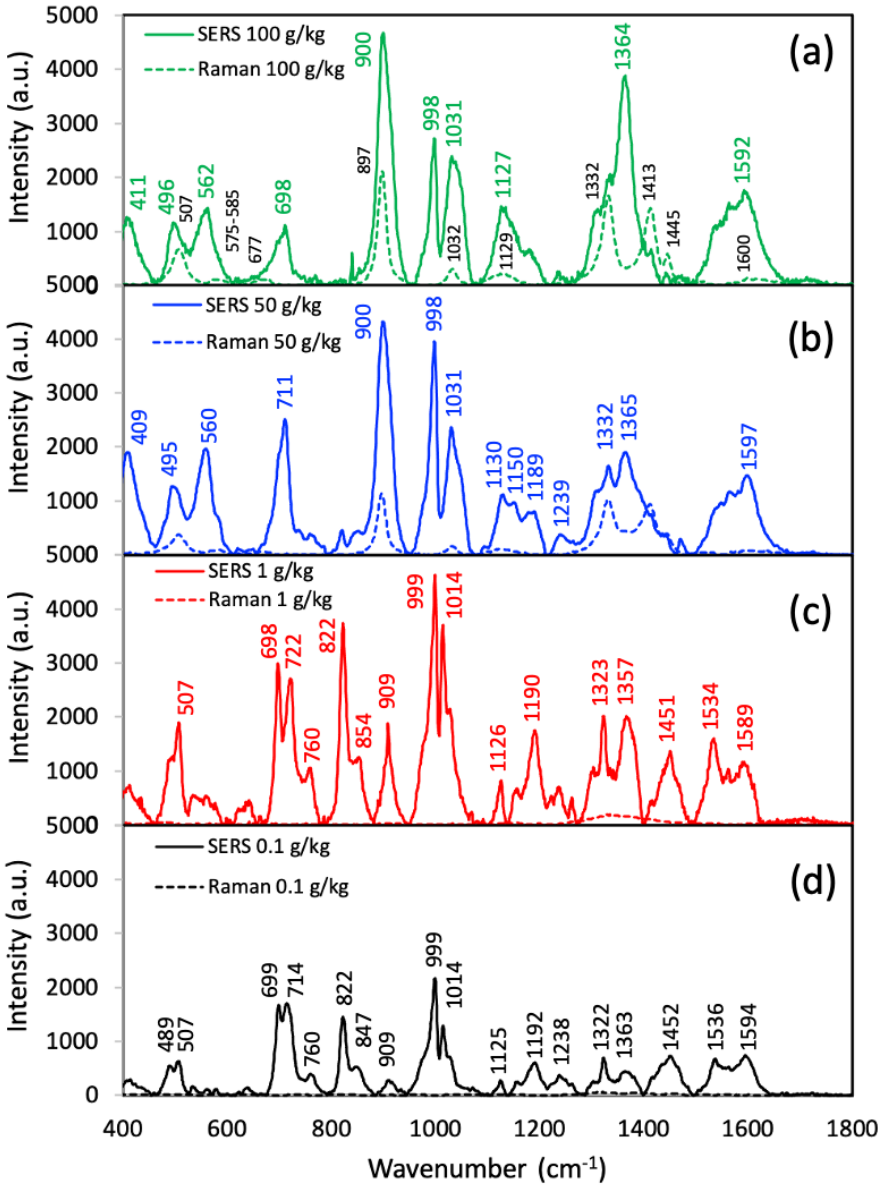

Figure 4: SERS (solid lines) and Raman (dashed lines) spectra of glycine solutions of concentration a) 100, b) 50 c) 1, and d) 0.1 g/kg at pH 4. The SERS spectra were acquired 60 min after solution preparation.

could also arise from the citrate functionalisation. In fact, when we consider the SERS signal from AuNPs in the absence of glycine (see Figure 5), we can see that the spectra for the lowest glycine concentration in Figure 4(d) appears to be dominated by the citrate contribution.

To interpret this further we have used the spectra in Figures 4 and 5 and literature assignments to attribute major peaks in the SERS spectra to glycine or citrate modes. The peak at 507 cm^{-1} appears in both the glycine Raman spectra and the NaCl SERS spectrum, so is likely to be due to a mode common to both molecules, which is consistent with a CO_2 rock [24] or CO_2 bend [28] mode. The peaks in the range 711 cm^{-1} to 854 cm^{-1} and the peak at 999 cm^{-1} appear in the SERS spectra for glycine and NaCl solutions but not in the Raman spectra of glycine, so are likely to be citrate C-C-C bending and C-C-C-C torsion modes. The peak at 900 cm^{-1} in the higher concentration glycine solutions is close to the 897 cm^{-1} peak in the glycine Raman spectra, which is attributed to a C-C stretch mode [24, 25]. The peak at 909 cm^{-1} that appears in the SERS NaCl solution and the lower concentration glycine solutions, is likely to be due to the

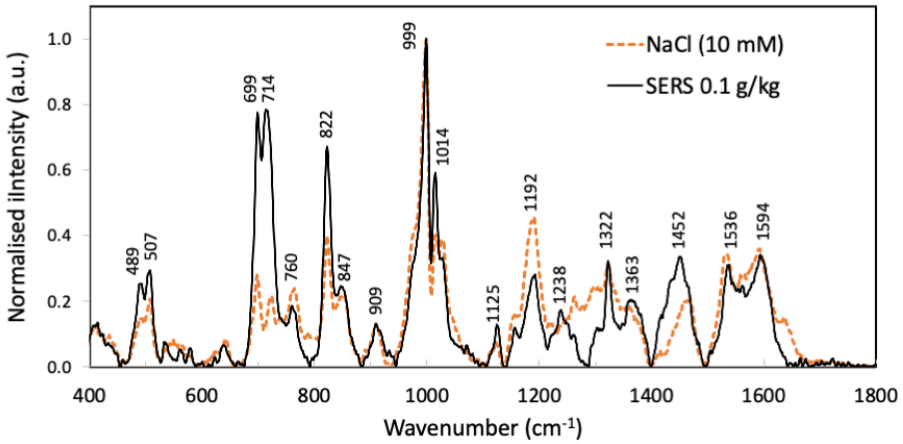

Figure 5: SERS spectra of a 0.1 g/kg glycine AuNP solution at pH 4, and a 10 mM NaCl AuNP solution at pH 4.13. Spectra intensities have been normalised so that the maximum intensities are equal. Frequency labels correspond to the SERS 0.1 g/kg spectrum.

same mode in the citrate molecule. The strong peak at 999 cm^{-1} is present in all SERS spectra, but not the glycine Raman spectra, and must be a citrate vibration. The peak at 1014 cm^{-1} only appears in the SERS spectra for the NaCl 10 mM and 0.1 and 1 g/kg glycine solutions and must also be a citrate vibration. These vibrations must be C-O or C-C-O stretches from the central hydroxyl group, which are not present in glycine. The C-C-O stretch is in the range 1000-1075 cm^{-1} for primary alcohols [29] and the C-O stretch is in the range 1000-1100 cm^{-1} for methanol and ethanol aqueous solutions [30]. The peak at 1032 cm^{-1} in the Raman spectra for glycine solutions also appears in SERS spectra for glycine but does not appear in the SERS spectra for the NaCl solution. It is, therefore, likely to be a C-N or NH_3 mode in glycine, which agrees with an assigned C_α-N stretch [25]. The peaks at 1129 and 1332 cm^{-1} appear in the Raman spectra of glycine solutions, and at similar wavenumbers in the SERS spectra for the glycine solutions and for the NaCl 10 mM solution, where glycine is not present. The modes can been attributed to C-C-H vibrations [25], CH_2 wag [24], respectively, which are common to both glycine and citrate. The peak at 1364 cm^{-1} in the SERS spectra for 100 g/kg glycine solution, appears at a similar wavenumber in the SERS spectra for all glycine concentrations. There is a broad band spanning this frequency in the SERS spectrum of the NaCl solution but it is not clearly present in the Raman spectra for glycine solutions, so it is likely to be a citrate vibration. The small peak at 1445 cm^{-1} in the Raman spectrum for glycine also appears in the SERS spectra for the lower glycine concentrations and is attributed to a CH_2 vibration [24, 25]. The peak at 1533 cm^{-1} appears in the SERS spectra for NaCl and the lower concentration glycine solutions but not in the SERS spectra for higher concentration glycine solutions or in the glycine Raman spectra. We, therefore attribute this to the citrate functionalisation. The SERS peak at 1589-1597 cm^{-1}, which is present in all SERS spectra, is close to the 1600 cm^{-1} peak in the glycine Raman spectra, that is attributed the COO asymmetric stretch in glycine [25], and is likely to also be a COO asymmetric stretch in citrate.

It is clear that the SERS spectra for lower glycine concentrations are dominated by citrate vibrations. Nevertheless, citrate peaks remain at higher glycine concentrations. For example, the citrate C-O or C-C-O stretch mode at 999 cm^{-1} is present in all SERS spectra in Figures 4 and 5. This shows that the proposed mechanism of aggregation is not due to glycine displacing citrate via competitive adsorption, and thus destabilisation of citrate covered AuNP must occur by glycine affecting citrate dissociation, as discussed in section 3.2. We also note that the 999 cm^{-1} peak is strongest for a glycine concentration of 1 g cm^{-3}, and starts to decrease in intensity as the glycine concentration increases, particularly for the 100 g cm^{-3} concentration. This decrease in intensity is likely to be due to sedimentation of the AuNP aggregates, however, we note that it is also possible that glycine molecules interact with the citrate functional groups and act to suppress citrate vibration modes as the glycine concentration increases.

To gain a better insight into the kinetics of AuNP aggregation and its effect on the SERS signal, we measured the SERS signal at 10-minute intervals after mixing. Directly after mixing the AuNPs have not significantly aggregated, as shown in Figure 3, therefore, we expect that at the point of mixing the SERS signal would be similar to the Raman signal. As aggregation progresses with time, the SERS signal would become stronger. Figure 6 shows the time evolution of the SERS spectra for a glycine concentration of 50 g/kg, which is a high enough concentration to show a Raman signal. As expected, the SERS spectrum directly after mixing (0 min) is very similar to the Raman spectrum. As aggregation progresses with time the SERS spectra increase in intensity. A similar growth in peak intensity with time is seen for 0.1 g/kg and 1 g/kg solutions. Although the Raman spectra for these concentrations are extremely weak, the SERS spectra at 0 minutes are already visible. Although UV Vis/DLS measurements did not show aggregation for the lowest concentration of 0.1 g/kg glycine (Figure 2(a)), the SERS signal at this concentration is consistent with the well known fact that SERS is very sensitive to the small amount of aggregation that can be observed in the UV Vis spectrum or that this is the signal from unaggregated AuNPs, dominated by citrate (see above). In Figure 5, we show the SERS signal for citrate covered AuNP in the presence of NaCl, which was used to aggregate the AuNP at pH 4, together with the SERS signal in the presence of 0.1 g/kg of glycine. Since these two spectra are very similar, this shows that the SERS signal measured at the lowest glycine concentration is primarily from the citrate, so the glycine is not displacing the citrate from the AuNP surface at this glycine concentration.

To more clearly see the change in SERS intensity with time we focused on the intensity of the peak at 900 cm^{-1}, which corresponds to a C-C stretch, for the 50 g/kg glycine solution (see Figure 6). The intensity of this peak increases with time continuously over the entire 60 minutes and the peak position shifts slightly to a higher wavenumber i.e. from 897 cm^{-1} to 900 cm^{-1} (see Supporting Information). This shift is likely to be due to the citrate C-C mode at 909 cm^{-1} strengthening as AuNP aggregation progresses, resulting in a broadened, asymmetric peak at 900 cm^{-1}. The variation of the maximum intensity of the peak at 900 cm^{-1}

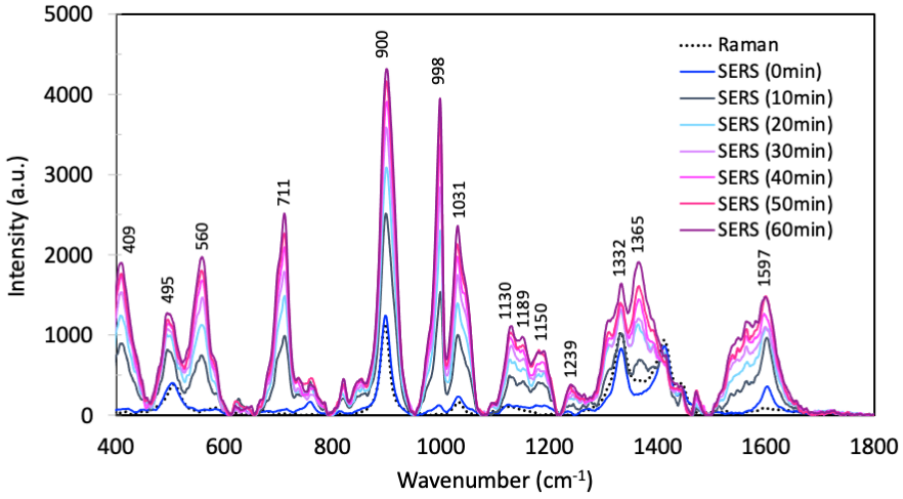

Figure 6: Time-dependent SERS and Raman spectra for 50 g/kg glycine solution at pH 4. Frequency labels correspond to the SERS (60 min) spectrum.

for all glycine concentrations with time is shown in Figure 7. For all concentrations, except for 100 g/kg, the measured SERS spectra (with AuNPs) directly after mixing (0 min) is similar to the Raman spectra (without AuNPs). For the 0.1 and 1 g/kg solutions there is a small increase in intensity, then the intensity plateaus after around 10 minutes, whereas the intensity for the 50 g/kg solution continues to increase for the full 60 minutes measured. For the highest concentration of 100 g/kg, the initial SERS intensity is several times greater than the Raman, indicating that aggregation has occurred extremely quickly. Although the hydrodynamic radius increases with time, the SERS spectra decreases in intensity with time. As previously discussed, this is likely to be due to sedimentation of AuNP aggregates out of solution, which lowers the

SERS intensity.

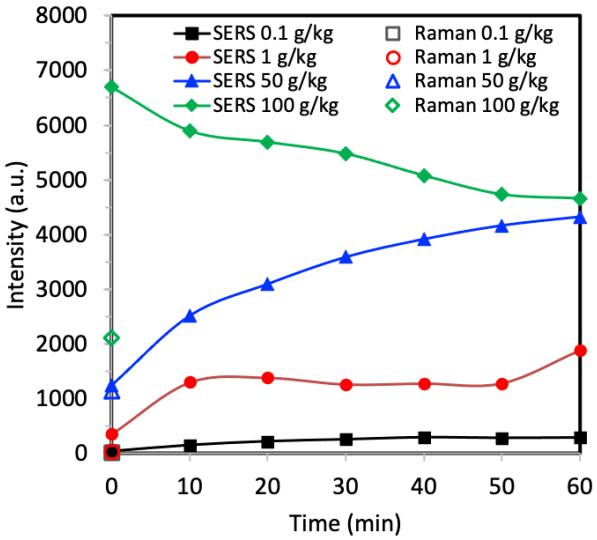

Figure 7: Effect of time and concentration of glycine on the intensity of the peak at 900 cm^{-1} in the SERS and Raman spectra.

To use SERS as a tool to study nucleation we need to investigate even higher glycine concentrations. There is clear sedimentation in the 100 g/kg glycine solution from UV Vis extinction and SERS spectra. However, this is not clear from DLS measurements, which indicates that DLS may not be able to measure very large aggregates that are slowly sedimenting (but not diffusing) [31] so DLS may not be a good measure for aggregation for concentrations higher than 50 g/kg at pH 4. In order to use SERS to investigate glycine solutions at higher concentrations we need to vary pH, to account for the interplay of surface charge of functionalised AuNP and the charge state of glycine. As we see in Supporting Information Figure SI.1, there is no aggregation detected by UV Vis extinction at the natural pH of 6.34 for glycine solutions at 50 g/kg, where the citrate approaches its full deprotonation as the highest pKa of citrate is 6.4. While NaCl is typically used to aggregate AuNPs, it is not desirable for nucleation studies as it is known to affect glycine nucleation [32]. In this work we show that it is possible to control aggregation of AuNPs without NaCl, using careful adjustment of pH and glycine concentration, which opens an avenue to use SERS to explore nucleation at interfaces between gold and aqueous glycine solutions.

4 Conclusions

We propose that SERS could be a useful interfacial probe to investigate local liquid composition and structure at solid-solution interfaces, where liquid mixture components are present at relatively high concentration. However, as the SERS measurements are very sensitive to the extent of AuNP aggregation, which itself is strongly dependent on the analyte concentration, it is imperative to understand and control how the solution concentration affects AuNP aggregration. This work investigated the aggregation of citrate-functionalised AuNPs under different pH and glycine concentrations and its effect on SERS measurements.

In the absence of glycine, UV-Vis extinction measurements showed that citrate-functionalised AuNPs did not aggregate for pH values of 4 or above, therefore a pH of 4 was used to investigate glycine aqueous solutions of different concentrations. It was found that increasing the glycine concentration increased the rate and extent of aggregation of AuNPs. UV Vis extinction measurements showed that there was very weak aggregation in the lower concentration glycine solutions of 0.1 and 1 g/kg, whereas there was a strong aggregation for 50 and 100 g/kg, consistent with DLS measurements of hydrodynamic diameter. Under these pH conditions glycine is zwitterionic, and its effect on the colloidal stability of AuNPs is most likely due to its association with citrate, affecting its charge state, resulting in reduction of the electrostatic stabilisation of the AuNPs.

SERS measurements of the solutions directly after solution preparation were very similar to Raman measurements (without AuNPs), and the SERS peaks developed as aggregation of AuNPs proceeded. The two lower concentration glycine solutions exhibited qualitatively different spectra to the two more concentrated glycine solutions. Comparison of these lower concentration solutions with SERS measurements of citrate-functionalised AuNP solutions, aggregated using NaCl and without glycine, revealed that the signal from the lower concentration glycine solutions was primarily due to the citrate functionalisation of the AuNP. SERS measurements of the higher concentration glycine solutions showed a combination of features from Raman of the bulk solution, as well as SERS from glycine and citrate.

Our results show that it is possible to control aggregation of AuNPs without the use of NaCl, using careful adjustment of pH and glycine concentration. This provides a novel way to use SERS as a tool to explore local solution structure and composition near gold interfaces, which is particularly important in understanding the mechanism of heterogeneous nucleation from solution.

Acknowledgements

We would like to thank The Carnegie Trust for the Universities of Scotland for funding this study (Grant ref: RIG007756). Jan Sefcik is grateful for support from the EPSRC Future Manufacturing Research Hub in Continuous Manufacturing and Advanced Crystallization (Grant ref: EP/P006965/1). Karen Faulds gratefully acknowledges funding from BBSRC (Grant ref: BB/R00899X/1) and from the Defence and Science Technology Laboratory.

Supporting Information

Raw experimental data are available at https://doi.org/10.15129.58530d44-5b40-42a5-ba5f-0ae45f1b1f89.

5 References

[1] Xiaoming Dou, Young Mee Jung, Hiroshi Yamamoto, Shigeru Doi, and Yukihiro Ozaki. Near-infrared excited surface-enhanced raman scattering of biological molecules on gold colloid i: Effects of ph of the solutions of amino acids and of their polymerization. *Applied Spectroscopy*, 53(2):133–138, 1999.

[2] Animesh K. Ojha, Patrice Donfack, and Arnulf Materny. Complex concentration dependence of sers and uv–vis absorption of glycine/ag-substrates because of glycine-mediated ag-nanostructure modifications. *Journal of Raman Spectroscopy*, 43(9):1183–1190, 2012.

[3] Xiaoming Dou, Young Mee Jung, Zhuang-Qi Cao, and Yukihiro Ozaki. Surface-enhanced raman scattering of biological molecules on metal colloid ii: Effects of aggregation of gold colloid and comparison of effects of ph of glycine solutions between gold and silver colloids. *Applied Spectroscopy*, 53(11):1440–1447, 1999.

[4] Alia Sabur, Mickael Havel, and Yury Gogotsi. Sers intensity optimization by controlling the size and shape of faceted gold nanoparticles. *Journal of Raman Spectroscopy*, 39(1):61–67, 2008.

[5] Edyta Podstawka, Yukihiro Ozaki, and Leonard M. Proniewicz. Part iii: Surface-enhanced raman scattering of amino acids and their homodipeptide monolayers deposited onto colloidal gold surface. *Appl. Spectrosc.*, 59(12):1516–1526, Dec 2005.

[6] J. S. Suh and M. Moskovits. Surface-enhanced raman spectroscopy of amino acids and nucleotide bases adsorbed on silver. *Journal of the American Chemical Society*, 108(16):4711–4718, 08 1986.

[7] John Turkevich, Peter Cooper Stevenson, and James Hillier. A study of the nucleation and growth processes in the synthesis of colloidal gold. *Discuss. Faraday Soc.*, 11:55–75, 1951.

[8] G. Frens. Controlled Nucleation for the Regulation of the Particle Size in Monodisperse Gold Suspensions. *Nature Physical Science*, 241(105):20–22, 1973.

[9] Hesham M. Zakaria, Akash Shah, Michael Konieczny, Joan A. Hoffmann, A. Jasper Nijdam, and M. E. Reeves. Small Molecule- and Amino Acid-Induced Aggregation of Gold Nanoparticles. *Langmuir*, 29(25):7661–7673, 06 2013.

[10] EV Boldyreva, VA Drebushchak, TN Drebushchak, IE Paukov, Yu A Kovalevskaya, and ES Shutova. Polymorphism of glycine, Part I. *Journal of Thermal Analysis and Calorimetry*, 73(2):409–418, 2003.

[11] K. Srinivasan. Crystal growth of and glycine polymorphs and their polymorphic phase transformations. *Journal of Crystal Growth*, 311(1):156 – 162, 2008.

[12] Anna Jawor-Baczynska, Jan Sefcik, and Barry D Moore. 250 nm glycine-rich nanodroplets are formed on dissolution of glycine crystals but are too small to provide productive nucleation sites. *Crystal growth & design*, 13(2):470–478, 2013.

[13] Jung F. Kang, Julien Zaccaro, Abraham Ulman, and Allan Myerson. Nucleation and growth of glycine crystals on self-assembled monolayers on gold. *Langmuir*, 16(8):3791–3796, 04 2000.

[14] Kimberley Allen, Roger J. Davey, Elena Ferrari, Christopher Towler, Gordon J. Tiddy, Merfyn O. Jones, and Robin G. Pritchard. The crystallization of glycine polymorphs from emulsions, microemulsions, and lamellar phases. *Crystal Growth & Design*, 2(6):523–527, 2002.

[15] In Sung Lee, Ki Tae Kim, Alfred Y. Lee, and Allan S. Myerson. Concomitant crystallization of glycine on patterned substrates: The effect of ph on the polymorphic outcome. *Crystal Growth & Design*, 8(1):108–113, 01 2008.

[16] Ensieh Seyedhosseini, Maxim Ivanov, Vladimir Bystrov, Igor Bdikin, Pavel Zelenovskiy, Vladimir Ya. Shur, Andrei Kudryavtsev, Elena D. Mishina, Alexander S. Sigov, and Andrei L. Kholkin. Growth and Nonlinear Optical Properties of β-Glycine Crystals Grown on Pt Substrates. *Crystal Growth & Design*, 14(6):2831–2837, 06 2014.

[17] Maria J. Vesga, David McKechnie, Paul A. Mulheran, Karen Johnston, and Jan Sefcik. Conundrum of γ glycine nucleation revisited: to stir or not to stir? *CrystEngComm*, 21:2234, 2019.

[18] David McKechnie, Samira Anker, Saraf Zahid, Paul A Mulheran, Jan Sefcik, and Karen Johnston. Interfacial concentration effect facilitates heterogeneous nucleation from solution. *J. Phys. Chem. Lett.*, 11(6):2263–2271, 2020.

[19] Juan Yguerabide and Evangelina E. Yguerabide. Light-scattering submicroscopic particles as highly fluorescent analogs and their use as tracer labels in clinical and biological applications: I. theory. *Analytical Biochemistry*, 262(2):137 – 156, 1998.

[20] Juan Yguerabide and Evangelina E. Yguerabide. Light-scattering submicroscopic particles as highly fluorescent analogs and their use as tracer labels in clinical and biological applications: Ii. experimental characterization. *Analytical Biochemistry*, 262(2):157 – 176, 1998.

[21] Jun Huang, Thomas C. Stringfellow, and Lian Yu. Glycine Exists Mainly as Monomers, Not Dimers, in Supersaturated Aqueous Solutions: Implications for Understanding Its Crystallization and Polymorphism. *J. Am. Chem. Soc.*, 130:13973–13980, 2008.

[22] Roy Govrin, Shani Tcherner, Tal Obstbaum, and Uri Sivan. Zwitterionic osmolytes resurrect electrostatic interactions screened by salt. *Journal of the American Chemical Society*, 140(43):14206–14210, 10 2018.

[23] Harsh Kumar, Meenu Singla, and Rajeev Jindal. Interactions of glycine, l-alanine and l-valine with aqueous solutions of trisodium citrate at different temperatures: A volumetric and acoustic approach. *The Journal of Chemical Thermodynamics*, 67:170 – 180, 2013.

[24] K. Furić, V. Mohaček, M. Bonifačić, and I. Štefanić. Raman spectroscopic study of h2o and d2o water solutions of glycine. *Journal of Molecular Structure*, 267:39 – 44, 1992. MOLECULAR SPECTROSCOPY AND MOLECULAR STRUCTURE 1991 Proceedings of the XXth European Congress on Molecular Spectroscopy.

[25] Najoua Derbel, Belén Hernández, Fernando Pflüger, Jean Liquier, Frédéric Geinguenaud, Nejmeddine Jaïdane, Zohra Ben Lakhdar, and Mahmoud Ghomi. Vibrational Analysis of Amino Acids and Short Peptides in Hydrated Media. I. L-glycine and L-leucine. *The Journal of Physical Chemistry B*, 111(6):1470–1477, 02 2007.

[26] Y. Ding and K. KroghJespersen. The 1:1 glycine zwitterionwater complex: An ab initio electronic structure study. *J. Comput. Chem.*, 17:338–349, 1996.

[27] S. G. Stepanian, I. D. Reva, E. D. Radchenko, M. T. S. Rosado, M. L. T. S. Duarte, R. Fausto, and L. Adamowicz. Matrix-isolation infrared and theoretical studies of the glycine conformers. *The Journal of Physical Chemistry A*, 102(6):1041–1054, 02 1998.

[28] Santosh Kumar, Amareshwar K. Rai, V.B. Singh, and S.B. Rai. Vibrational spectrum of glycine molecule. *Spectrochimica Acta Part A: Molecular and Biomolecular Spectroscopy*, 61(11):2741 – 2746, 2005.

[29] Brian C. Smith. The C-O Bond, Part I: Introduction and the Infrared Spectroscopy of Alcohols. *Spectroscopy*, 32(1):14–21, 2017.

[30] M. Khalique Ahmed, Sheikh Ali, and Ewa Wojcik. The c-o stretching infrared band as a probe of hydrogen bonding in ethanol–water and methanol–water mixtures. *Spectroscopy Letters*, 45(6):420–423, 2012.

[31] Hua Wu, Marco Lattuada, Peter Sandkühler, Jan Sefcik, and Massimo Morbidelli. Role of sedimentation and buoyancy on the kinetics of diffusion limited colloidal aggregation. *Langmuir*, 19(26):10710–10718, 12 2003.

[32] Xia Yang, Jie Lu, Xiu-Juan Wang, and Chi-Bun Ching. Effect of sodium chloride on the nucleation and polymorphic transformation of glycine. *Journal of Crystal Growth*, 310(3):604 – 611, 2008.